Inorg. Chem. **2002**, *41*, 3429–3436

A Study of Structural and Bonding Variations in the Homologous Series $[Mo_2(CN)_6(dppm)_2]^{n-}$ (n = 2, 1, 0)

Jitendra K. Bera, Paul S. Szalay, and Kim R. Dunbar*

Department of Chemistry, Texas A&M University, P.O. Box 30012, College Station, Texas 77842-3012

Received February 26, 2002

Reaction of $Mo_2Cl_4(dppm)_2$ (dppm = bis(diphenylphosphino)methane) with 6 equiv of [*n*-Bu_4N][CN] or [Et_4N][CN] in dichloromethane yields [*n*-$Bu_4N]_2[Mo_2(CN)_6(dppm)_2]$ (**1**) and [$Et_4N]_2[Mo_2(CN)_6(dppm)_2]$ (**2**), respectively. The corresponding one- and two-electron oxidation products [*n*-$Bu_4N][Mo_2(CN)_6(dppm)_2]$ **(3)** and $Mo_2(CN)_6(dppm)_2$ **(4)** were prepared by reactions of **1** with the oxidant $NOBF_4$. Single-crystal X-ray structures of **2**·$2CH_3CN$, **3**·$2CH_3CN$·$2H_2O$, and **4**·$2CH_3NO_2$ were performed, and the results confirmed that all three complexes contain identical ligand sets with *trans* dppm ligands bisecting the $Mo_2(\mu\text{-}CN)_2(CN)_4$ equatorial plane. The binding of the bridging cyanide ligands is affected by the oxidation state of the dimolybdenum core as evidenced by an increase in side-on π-bonding overlap of the μ-CN in going from **1** to **4**. The greater extent of π-donation into Mo orbitals is accompanied by a lengthening of the Mo–Mo distance (2.736(1) Å in $Mo_2^{II,II}$ (**2**), 2.830(1) Å in $Mo_2^{II,III}$ (**3**), and 2.936(1) Å in $Mo_2^{III,III}$ (**4**)). A computational study of the closed-shell members of this homologous series, $[Mo_2(CN)_6(dppm)_2]^n$ (n = 2–, 0), indicates that the more pronounced side-on π-donation evident in the X-ray structure of **4** leads to significant destabilization of the δ orbital and marginal stabilization of the δ^* orbitals with respect to nearly degenerate δ and δ* orbitals in the parent compound, **2**. The loss of δ contributions combined with the reduced orbital overlap due to higher charges on molybdenum centers in oxidized complexes **3** and **4** is responsible for the observed increase in the length of the Mo–Mo bond.

Introduction

Cyanide chemistry is one of the oldest and richest areas of classical coordination chemistry, dating back to 1704 when the German artist Diesbach discovered the mixed-valence iron(III) hexacyanoferrate(II) compound $Fe_4[Fe(CN)_6]_3 \cdot xH_2O$, known as Prussian blue.[1] Over the course of the three centuries since this finding, a large body of experimental data has been amassed regarding the synthesis and characterization of transition metal cyanide compounds and solid-state materials.[2] One aspect of cyanide chemistry, however, that has witnessed relatively little development to date is the area of low-valent transition metal compounds of cyanide with metal−metal bonds, a situation that has sparked our interest.[3] At the time we embarked on this project several years ago, the only dinuclear M−M bonded cyanide compounds reported in the literature were $K[Mo_2(\mu\text{-}CN)(CO)_4(Cp)_2]$,[4] $Mn_2(\mu\text{-}CN)H(CO)_5(dppm)_2$,[5] [*n*-$Bu_4N]_n[M_2(\mu\text{-}CN)(OR)_6]$[6] ($n$ = 1, 2) (M = Mo or W), and $[Rh_2(\mu\text{-}CN)(\mu\text{-}$

* To whom correspondence should be addressed. E-mail: dunbar@mail.chem.tamu.edu. Fax: (+1) 979-845-7177.

(1) (a) Keggin, J. F.; Miles, F. D. *Nature*, **1936**, *137*, 577. (b) Prandtl, W.; Mohr, S. *Z. Anorg. Allg. Chem.* **1938**, *236*, 243. (c) Holtzman, H. *Ind. Eng. Chem.* **1945**, *37*, 855. (d) Dows, D. A.; Haim, A.; Wimarth, W. K. *J. Inorg. Nucl. Chem.* **1961**, *21*, 33.

(2) (a) Vahrenkamp, H.; Geiss, A.; Richardson, G. N. *J. Chem. Soc., Dalton Trans.* **1997**, *20*, 3664. (b) Heintz, R. A.; Dunbar, K. R. *Prog. Inorg. Chem.* **1996**, *45*, 283. (c) Sharpe, A. G. In *The Chemistry of Cyano Complexes of the Transition Metals*; Maitlis, P. M., Stone, F. G. A., West, R., Eds.; Academic: New York, 1976. (d) Griffith, W. P. *Coord. Chem. Rev.* **1975**, *17*, 177.

(3) (a) A variety of cyanide-containing cluster compounds have been reported in recent years. See for examples: (a) Naumov N. G.; Soldatov D. V.; Ripmeester J. A.; Artemkina S. B.; Fedorov V. E. *Chem. Commun.* **2001**, 571. (b) Mironov, Y. V.; Virovets, A. V.; Sheldrick, W. S.; Fedorov, V. E. *Polyhedron* **2001**, *20*, 969. (c) Elsegood, M. R. J.; Virovets A. V.; Samsonenko, D. G.; Kalinina, I. V.; Fedin, V. P. *J. Struct. Chem.* **2000**, *41*, 1073. (d) Fedin, V. P.; Virovets A. V.; Kalinina, I. V.; Ikorskii, V. N.; Elsegood, M. R. J.; Clegg, W. *Euro. J. Inorg. Chem.* **2000**, *11*, 2341. (e) Fedin, V. P.; Kalinina, I. V.; Samsonenko, D. G.; Mironov, Y. V.; Sokolov, M. N.; Tkachev, S. V.; Naumov, N. G.; Artemkina, S. B.; Virovets, A. V.; Fedorov, V. E. *J. Solid State Chem.* **2000**, *153*, 195. (f) Mironov, Y. V.; Virovets, A. V.; Naumov, N. G.; Ikorskii, V. N.; Fedorov, V. E. *Chem. Eur. J.* **2000**, *6*, 1361. (g) Magliocchi, C.; Xie, X. B.; Hughbanks, T. *Inorg. Chem.* **2000**, *39*, 5000. (h) Virovets, A. V.; Podberezskaya, N. V.; Elsegood, M. R. J.; Clegg, W.; Sykes, A. G. *Inorg. Chem.* **1999**, *38*, 1956.

(4) Curtis, M. D.; Klinger, R. J. *J. Organomet. Chem.* **1978**, *161*, 23.

10.1021/ic020157n CCC: $22.00
Published on Web 06/06/2002

$CO)(CO)_2(dppm)_2][ClO_4]_2$.[7] Our initial foray into this area of chemistry led to the X-ray characterization of the first homoleptic M−M bonded cyanide compound, $[Mo_2(CN)_8]^{4-}$. The related compound, $[Mo_2(CN)_6(O_2CCH_3)]^{3-}$, was also isolated and fully characterized.[8] In an attempt to prepare $Re_2(CN)_4(dppm)_2$ by metathetic displacement of Cl^- with CN^- ligands from $Re_2Cl_4(dppm)_2$, we discovered that the unprecedented edge-sharing bioctahedral (ESBO) anion $[Re_2(CN)_6(dppm)_2]^{2-}$ was formed instead.[8] This type of reaction appears to be quite general, as evidenced by the fact that the corresponding anion $[Mo_2(CN)_6(dppm)_2]^{2-}$ is readily prepared from $Mo_2Cl_4(dppm)_2$, a result that was recently communicated by our group.[9]

We now report the isolation and full characterization of the two-electron oxidation products of $[Mo_2(CN)_6(dppm)_2]^{2-}$. An improved structure solution of the $[Mo_2(CN)_6(dppm)_2]^{2-}$ unit is also included. The influence of the metal oxidation state and the bridging cyanide binding mode on the Mo−Mo bonding in the homologous series $[Mo_2(CN)_6(dppm)_2]^{2-}$, $[Mo_2(CN)_6(dppm)_2]^{1-}$, and $Mo_2(CN)_6(dppm)_2$ was probed by examining the structural parameters of all three compounds in the solid state,[10,11] and by performing computational studies on the two closed-shell members of the series, $[Mo_2(CN)_6(dppm)_2]^{2-}$ and $Mo_2(CN)_6(dppm)_2$.

Experimental Section

Materials. All manipulations were carried out under an inert atmosphere with the use of standard drybox and Schlenk-line techniques. Glassware was flame-dried under vacuum prior to use. Dichloromethane, acetonitrile, and diethyl ether were dried by conventional methods, distilled over nitrogen, and deoxygenated prior to use. $Mo_2Cl_4(dppm)_2$ was prepared according to the literature method.[12] The reagent $NOBF_4$ was purchased from Aldrich and used without further purification whereas $[Cp_2Fe][BF_4]$ was prepared according to a literature method.[13]

Physical Measurements. Infrared spectra were recorded in the range 4000−400 cm^{-1} on a Nicolet IR/42 spectrometer using Nujol mulls on KBr plates. The ^1H and ^{31}P NMR spectra were recorded on a Varian VXR 300s spectrometer. Electronic absorption and near-IR spectra were measured on a Shimadzu UV-3101PC UV−vis−NIR scanning spectrophotometer. Cyclic voltammetric studies were carried out with a CH Instruments electrochemical workstation in 0.1M $[n\text{-}Bu_4N][PF_6]/CH_3CN$ solutions at a Pt disk working electrode with a Pt wire auxiliary electrode and Ag/AgCl reference. Elemental analyses were performed on a Perkin-Elmer Series II CHNS/O analyzer. Mass spectral data were obtained at the Michigan State University Mass Spectrometry Facility which is supported, in part, by a grant (DRR-00480) from the Biotechnology Research Technology Program, National Center for Research Resources, National Institute of Health.

Syntheses. Preparation of $[n\text{-}Bu_4N]_2[Mo_2(CN)_6(dppm)_2]$ (1). A mixture of $Mo_2Cl_4(dppm)_2$ (0.200 g, 0.181 mmol) and $[n\text{-}Bu_4N][CN]$ (0.292 g, 1.087 mmol) was stirred in 15 mL of dichloromethane for 6−8 h. The resulting dark red solution was concentrated, and 10 mL of diethyl ether was added to induce precipitation of a dark red microcrystalline solid. The product was collected by filtration, washed with diethyl ether (3 × 5 mL), and dried in vacuo. Yield: 0.145 g (50%). Anal. Calcd for $C_{88}H_{114}N_8P_4Mo_2$: C, 66.01; H, 7.25; N, 7.00. Found: C, 65.18; H, 7.33; N, 6.58. ^1H NMR (CD_3CN): δ 4.08 ppm (2 H, pentet, $-CH_2-$ protons of dppm), δ 6.96 and 7.60 ppm (20 H, multiplets, phenyl protons of dppm). $^{31}P\{^1H\}$ NMR: δ 25.47 ppm. IR (KBr) data (cm^{-1}): ν_{CN} 2094, 2080, and 1936. UV−vis (CH_3CN) λ_{max}(nm) (ϵ (M^{-1} cm^{-1})): 553 (1.9×10^3), 333 (3.4×10^5).

Preparation of $[Et_4N]_2[Mo_2(CN)_6(dppm)_2]$ (2). A mixture of $Mo_2Cl_4(dppm)_2$ (0.112 g, 0.102 mmol) and $[Et_4N][CN]$ (0.114 g, 0.73 mmol) was stirred in 15 mL of dichloromethane for 6−8 h. The red solid obtained was filtered, washed with dichloromethane (3 × 5 mL), and dried in vacuo. Yield: 0.087 g (62%). Anal. Calcd for $C_{72}H_{84}N_8P_4Mo_2$: C, 62.79; H, 6.15; N, 8.14. Found: C, 63.03; H, 6.27; N, 7.82.

Preparation of $[n\text{-}Bu_4N][Mo_2(CN)_6(dppm)_2]$ (3). Method I: An acetonitrile solution (10 mL) of $NOBF_4$ (0.015 g, 0.123 mmol) was added dropwise into a stirring acetonitrile (10 mL) solution of **1** (0.165 g, 0.103 mmol) at −15 °C (ethylene glycol/dry ice bath). After complete addition of the $NOBF_4$ solution, the resulting green solution was allowed to warm to room temperature. The volume was reduced to 10 mL, filtered through Celite, and treated with diethyl ether (10 mL) to induce precipitation. The resulting green solid was collected by filtration, washed with portions of a 35/65 acetonitrile/diethyl ether mixture (3 × 5 mL), and dried in vacuo. Yield: 0.112 g (80%). Anal. Calcd for $C_{72}H_{80}N_7P_4Mo_2$: C, 64.28; H, 5.95; N, 7.29. Found: C, 63.89; H, 6.17; N, 6.98. IR(KBr) data (cm^{-1}): ν_{CN} 2108 and 1807 cm^{-1}. UV−vis (CH_3CN): λ_{max}(nm) (ϵ (M^{-1} cm^{-1})) 429 (800), 780 (1.2×10^3).

Method II: In an alternate method, $[n\text{-}Bu_4N][Mo_2(CN)_6(dppm)_2]$ (**3**) was prepared by reacting **1** (0.144 g, 0.09 mmol) with $[Cp_2Fe][BF_4]$ (0.026 g, 0.094 mmol). An acetonitrile solution of $[Cp_2Fe][BF_4]$ (10 mL) was added dropwise into a stirring acetonitrile (10 mL) solution of **1** that had been cooled to −15 °C in an ethylene glycol/dry ice bath. The resulting green solution was slowly warmed to room temperature, concentrated to 10 mL, and then filtered through Celite. Diethyl ether (10 mL) was added to precipitate a green solid that was recovered by filtration, washed with portions of a 35/65 acetonitrile/diethyl ether solution (3 × 5 mL), and dried in vacuo. Yield: 0.098 g (80%).

Preparation of $Mo_2(CN)_6(dppm)_2$ (4). An acetonitrile solution (20 mL) of $NOBF_4$ (0.026 g, 0.227 mmol) was added dropwise into a stirring acetonitrile (10 mL) solution of **1** (0.165 g, 0.103 mmol) in a round-bottomed flask that had been cooled to −15 °C in an ethylene glycol/dry ice bath. The reaction mixture was allowed to warm to room temperature. The solution was filtered through Celite and concentrated to 10 mL which led to the precipitation of a yellow-green solid. The product was collected by filtration, washed with acetonitrile (3 × 5 mL), and finally dried in vacuo. Yield: 0.080 g (70%). Anal. Calcd for $C_{56}H_{44}N_6P_4Mo_2$: C, 60.23; H, 3.97; N, 7.53. Found: C, 61.09; H, 4.25; N, 7.32. IR data (cm^{-1}): ν_{CN} 2110, 2102, and 1807 cm^{-1}.

Michigan State University Mass Spectrometry Facility which is supported, in part, by a grant (DRR-00480) from the Biotechnology Research Technology Program, National Center for Research Resources, National Institute of Health.

(5) Aspinall, H. C.; Deeming, A. J.; Donovan-Mtunzi, S. *J. Chem. Soc., Dalton Trans.* **1983**, *84*, 205.
(6) Budzichowski, T.; Chisholm, M. *Polyhedron*, **1994**, *13*, 2035.
(7) Deraniyag, S. P.; Grundy, K. R. *Inorg. Chim. Acta*, **1984**, *84*, 205.
(8) Bartley, S. L.; Bernstein, S. N.; Dunbar, K. R. *Inorg. Chim. Acta* **1993**, *213*, 213.
(9) Szalay, P. S.; Dunbar, K. R. *Inorg. Chem. Commun.* **2000**, *3*, 49.
(10) (a) Canich, J. A. M.; Cotton, F. A.; Dunbar, K. R.; Falvello, L. R. *Inorg. Chem.* **1988**, *27*, 804. (b) Canich, J. A. M.; Cotton, F. A.; Daniels, L. M.; Lewis, D. B. *Inorg. Chem.* **1987**, *26*, 4046. (c) Cotton, F. A. *Polyhedron*, **1987**, *6*, 667. (d) Chakravarty, A. R.; Cotton, F. A.; Diebold, M. P.; Lewis, D. B.; Roth, W. J. *J. Am. Chem. Soc.* **1986**, *108*, 971.
(11) Cotton, F. A.; Walton, R. A. *Multiple Bonds Between Metal Atoms*, 2nd ed.; Clarendon Press: Oxford, 1993.
(12) Green, M. L. H.; Parkin, G. *J. Chem. Soc., Dalton Trans.* **1982**, 2519.
(13) Hendrickson, D. N.; Sohn, Y. S.; Gray, H. B. *Inorg. Chem.* **1971**, *10*, 1559.

Table 1. Crystallographic Data for $[Et_4N]_2[Mo_2(CN)_6(dppm)_2]$ (**2**·$2CH_3CN$), $[n\text{-}Bu_4N][Mo_2(CN)_6(dppm)_2]$ (**3**·$2CH_3CN·2H_2O$), and $Mo_2(CN)_6(dppm)_2$ (**4**·$2CH_3NO_2$)

	2·$2CH_3CN$	**3**·$2CH_3CN·2H_2O$	**4**·$2CH_3NO_2$
formula	$C_{38}H_{45}N_5P_2Mo$	$C_{76}H_{90}N_9P_4O_2Mo_2$	$C_{58}H_{50}N_8P_4O_4Mo_2$
fw	729.67	1477.33	1238.82
space group	$P2_1/n$	$C2/c$	$P\bar{1}$
a (Å)	15.948(3)	27.353(6)	9.942(2)
b (Å)	13.203(3)	10.741(2)	12.418(3)
c (Å)	17.581(4)	26.149(5)	12.934(3)
α (deg)	90.00	90.00	95.47(3)
β (deg)	100.45(3)	107.50(3)	107.12(3)
γ (deg)	90.00	90.00	91.86(3)
V (Å^3)	3640.5(13)	7327(3)	1516.1(5)
Z	4	4	1
ρ_{calcd} (g/cm^3)	1.331	1.339	1.357
μ (Mo Kα) (cm^{-1})	48.2	48.1	56.9
temp, K	110 (2)	173 (2)	173 (2)
reflns collected	23245	22062	18034
independent	8709	8462	7021
obsd [$I > 2\sigma(I)$]	3188	5951	4948
no. variables	441	601	355
R1[a]	0.0575	0.0602	0.0423
wR2[b]	0.1108	0.1166	0.1049
GOF	0.759	1.052	0.904

[a] $R1 = \sum||F_o| - |F_c||/\sum|F_o|$ with $F_o^2 > 2\sigma(F_o^2)$. [b] $wR2 = [\sum w(|F_o^2| - |F_c^2|)^2/\sum|F_o^2|^2]^{1/2}$.

X-ray Crystallographic Studies. Single-crystal X-ray structural studies were performed on a Bruker SMART 1K CCD platform diffractometer with graphite monochromated Mo Kα radiation ($\lambda_\alpha = 0.71069$ Å). The frames were integrated in the Bruker SAINT software package,[14] and the data were corrected for absorption using the SADABS program.[15] The structures were solved and refined using the suite of programs in the SHELXTL V.5.10 package.[16] Pertinent crystallographic data for $[Et_4N]_2[Mo_2(CN)_6(dppm)_2]$ (**2**·$2CH_3CN$), $[n\text{-}Bu_4N][Mo_2(CN)_6(dppm)_2]$ (**3**·$2CH_3CN·2H_2O$), and $Mo_2(CN)_6(dppm)_2$ (**4**·$2CH_3NO_2$) are summarized in Table 1.

$[Et_4N]_2[Mo_2(CN)_6(dppm)_2]$, 2·$2CH_3CN$. Crystals of **2**·$2CH_3CN$ were grown by slow diffusion of ether into an acetonitrile solution of **2**. A dark red crystal of dimensions 0.49 × 0.41 × 0.09 mm^3 was covered in Paratone oil, mounted on the tip of a glass fiber, and secured with silicone grease. The cell constants and orientation matrix for data collection corresponded to a monoclinic cell. A total of 8709 unique reflections was collected at 110 K using the ω-scan technique to a maximum 2θ value of 57°. The space group was determined to be $P2_1/n$. All non-hydrogen atoms were refined with anisotropic thermal parameters. Hydrogen atoms were included in the final stages of the refinement as riding atoms at calculated positions.

$[n\text{-}Bu_4N][Mo_2(CN)_6(dppm)_2]$, 3·$2CH_3CN·2H_2O$. Crystals of **3**·$2CH_3CN·2H_2O$ were grown by slow evaporation of a benzene and acetonitrile solution of **1** in air. A green crystal of dimensions 0.38 × 0.25 × 0.07 mm^3 was covered in Paratone oil and mounted on the tip of a glass fiber with silicone grease. The cell constants and orientation matrix for data collection corresponded to a monoclinic cell. A total of 8462 unique reflections was collected at 173 K using the ω-scan technique to a maximum 2θ value of 56°. The space group was determined to be $C2/c$. All non-hydrogen atoms were refined with anisotropic thermal parameters. The hydrogen atoms were located from the difference map and were refined isotropically. The O1−H1WA and O1−H1WB distances were restrained to 0.85 Å.

$Mo_2(CN)_6(dppm)_2$, 4·$2CH_3NO_2$. Crystals of **4**·$2CH_3NO_2$ were grown in an 8 mm o.d. glass tube by slow diffusion of acetonitrile into a nitromethane solution of **4**. A yellow-green crystal of dimensions 0.42 × 0.35 × 0.28 mm^3 was covered in Paratone oil and mounted on the tip of a glass fiber with silicone grease. The cell constants and orientation matrix for data collection corresponded to a triclinic cell. A total of 7021 unique reflections was collected at 173 K using the ω-scan technique to a maximum 2θ value of 56°. The space group was determined to be $P\bar{1}$. All non-hydrogen atoms were refined with anisotropic thermal parameters. Hydrogen atoms were added in calculated positions and treated as riding atoms.

Theoretical Methods. Density functional theory (DFT) calculations were performed using the Gaussian-98 (G98)[17] suite of programs with Becke's three parameter hybrid exchange functional[18] and the Lee−Yang−Parr correlation functional[19] (B3LYP). A quasirelativistic effective core potential (ECP) with a small core (1s 2s 2p 3s 3p 3d) and double ξ basis set of Hay and Wadt[20] was used for Mo in conjunction with a Dunning basis set on H, C, and N.[21] LANL2DZ bases as implemented in G98 were used for P atoms with a small ECP core (1s 2s 2p). A d-polarization function was supplied for the P atoms.[22] All the calculations were performed with geometrical parameters taken from the single-crystal X-ray structures, except that the phenyl rings of the dppm ligands were replaced by hydrogen atoms at P−H distances of 1.40 Å. The multiplicities ($2S + 1$) were restricted to 1. The Cerius2[23] program was used to generate the graphic images of the molecular orbitals.

Results and Discussion

Synthetic Details. Several years ago, we reported that the reaction of $Re_2Cl_4(dppm)_2$ with cyanide leads to the formation of the anion $[Re_2(CN)_6(dppm)_2]^{2-}$, the first cyanide complex of the edge-sharing bioctahedral (ESBO) type. We later discovered that the salt $[n\text{-}Bu_4N]_2[Mo_2(CN)_6(dppm)_2]$ (**1**) was readily synthesized from a similar route, namely the reaction of $Mo_2Cl_4(dppm)_2$ with 6 equiv of CN^- in dichloromethane. In these reactions, the four terminal Cl^- ligands are replaced by CN^-, and two additional CN^- bridging ligands have been added. Fast-atom bombardment (FAB) mass spectrometry studies in both nitrobenzyl alcohol and glycerol matrixes were conducted to investigate the pos-

(14) *Saint 1000*; Bruker Analytical X-ray Instruments: Madison, WI, 1999.
(15) Sheldrick, G. M. *SABABS, Siemens Area Detector Absorption Correction*; University of Gottingen: Gottingen, Germany, 1998.
(16) *SHELTXL version 5.10, Reference Manual*; Bruker Industrial Automation, Analytical Instrument: Madison, WI, 1999.
(17) Frisch, M. J.; Trucks, G. W.; Schlegel, H. B.; Scuseria, G. E.; Robb, M. A.; Cheeseman, J. R.; Zakrzewski, V. G.; Montgomery, J. A., Jr.; Stratmann, R. E.; Burant, J. C.; Dapprich, S.; Millam, J. M.; Daniels, A. D.; Kudin, K. N.; Strain, M. C.; Farkas, O.; Tomasi, J.; Barone, V.; Cossi, M.; Cammi, R.; Mennucci, B.; Pomelli, C.; Adamo, C.; Clifford, S.; Ochterski, J.; Petersson, G. A.; Ayala, P. Y.; Cui, Q.; Morokuma, K.; Malick, D. K.; Rabuck, A. D.; Raghavachari, K.; Foresman, J. B.; Cioslowski, J.; Ortiz, J. V.; Stefanov, B. B.; Liu, G.; Liashenko, A.; Piskorz, P.; Komaromi, I.; Gomperts, R.; Martin, R. L.; Fox, D. J.; Keith, T.; Al-Laham, M. A.; Peng, C. Y.; Nanayakkara, A.; Gonzalez, C.; Challacombe, M.; Gill, P. M. W.; Johnson, B. G.; Chen, W.; Wong, M. W.; Andres, J. L.; Head-Gordon, M.; Replogle, E. S.; Pople, J. A. *Gaussian 98*; Gaussian, Inc.: Pittsburgh, PA, 1998.
(18) Becke, A. D. *J. Chem. Phys.* **1993**, *98*, 5648.
(19) Lee, C.; Yang, W.; Parr, R. G. *Phys. Rev.* **1988**, *37*, 785.
(20) (a) Hay, P. J.; Wadt, W. R. *J. Chem. Phys.* **1985**, *82*, 270. (b) Hay, P. J.; Wadt, W. R. *J. Chem. Phys.* **1985**, *82*, 284. (c) Hay, P. J.; Wadt, W. R. *J. Chem. Phys.* **1985**, *82*, 299.
(21) Dunning, T. H., Jr.; Hay, P. J. In *Modern Theoretical Chemistry*; Schaefer, H. F., III, Ed.; Plenum: New York, 1977; Vol. 3, p 1.
(22) Höllwarth, A.; Böhme, M.; Dapprich, S.; Ehlers, A. W.; Gobbi, A.; Jonas, V.; Köhler, K. F.; Stegmann, R.; Veldkamp, A.; Frenking, G. *Chem. Phys. Lett.* **1993**, *208*, 237.
(23) *Cerius 2*, version 3.5; Molecular Simulations Inc., 1997.

sibility of incomplete cyanide/chloride metathesis. A peak at *m*/*z* 1360, corresponding to the ion $[HMo_2(CN)_6(dppm)_2]^{1-}$, was observed in the FAB mass spectrum of **1** recorded in the negative ion mode. There was no evidence for the characteristic isotope pattern of chlorine. The establishment of the lack of chloride impurities in **1** ensures that any derivatives prepared from it will also be free of chloride ligands.

The original crystal structure of **1** reported in the communication[9] was based on a poor quality data set. One consequence of this situation is that the carbon and nitrogen atoms of the bridging cyanides exhibited a high degree of thermal motion. We recognized that the bridging C−N distance of 1.028(12) Å calculated from this data set is unreasonably short and proposed that the atoms were involved in a librational disorder,[24] a term that refers to oscillations of a bonded atom or atoms along an arc. Another possible cause of the poor refinement in the region of the bridging CN ligands is that the crystal contained the anion $[Mo_2^{II,II}(CN)_6(dppm)_2]^{2-}$ along with small quantities of the oxidized form $[Mo_2^{II,III}(CN)_6(dppm)_2]^{1-}$. The extreme sensitivity of $[Mo_2^{II,II}(CN)_6(dppm)_2]^{2-}$ toward air and moisture could have produced crystals resulting from a cocrystallization of the $Mo_2^{II,II}$ and the $Mo_2^{II,III}$ analogues which would render the refinement of the bridging cyanide positions invalid because their binding modes are sensitive to oxidation state. Indeed, the entire refinement of **1** would be compromised by this situation. In an attempt to avoid adventitious H_2O which is virtually impossible to do with the [*n*-Bu_4N][CN] reagent, the new salt $[Et_4N]_2[Mo_2(CN)_6(dppm)_2]$ (**2**) was prepared with very dry [Et_4N][CN], and a new X-ray structure was performed. The results described in full in the following sections indicate that the poor quality of the data and refinement has been eliminated with the use of the $[Et_4N]^+$ cation.

We note that **2** is insoluble in CH_2Cl_2, unlike **1**, and that a CH_3CN solution of **2** slowly decomposes over a long period of time in the absence of excess CN^-. A small amount of [Et_4N][CN] was added to the solution of **2** for growing single crystals.

Electrochemical and Chemical Oxidation of [*n*-Bu_4N]$_2$[$Mo_2(CN)_6(dppm)_2$] (1). A cyclic voltammetric study of **1** in 0.1 M $TBAPF_6/CH_3CN$ revealed the presence of two distinct one-electron oxidation couples located at $E_{1/2}(ox) = +0.29$ (60) V and +0.45 (70) V versus Ag/AgCl.[25] A reduction process at $E_{1/2}(red) = -0.49$ (60) V was also observed. The separation of 160 mV between the two oxidation processes was interpreted as a good indication that chemical methods to prepare the $Mo_2^{II,III}$ and $Mo_2^{III,III}$ species would be successful. Indeed, the one-electron oxidation product **3** was prepared in high yields by treating an acetonitrile solution of **1** with 1.2 equiv of $NOBF_4$ or [Cp_2Fe][BF_4] at −15 °C. The two-electron oxidation product **4** was prepared under analogous conditions by using 2.2 equiv of $NOBF_4$.

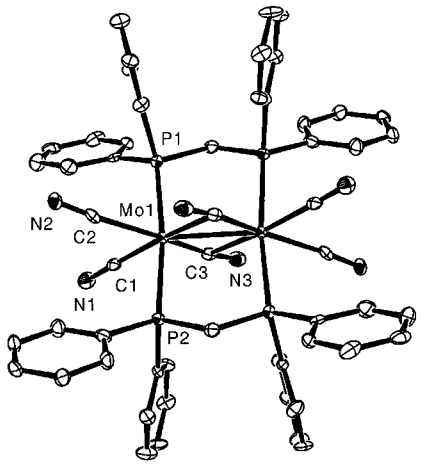

Figure 1. Thermal ellipsoid plot of the dianionic unit in $[Et_4N]_2[Mo_2(CN)_6(dppm)_2]$ (**2**·$2CH_3CN$) represented at the 50% probability level. Hydrogen atoms have been omitted for the sake of clarity.

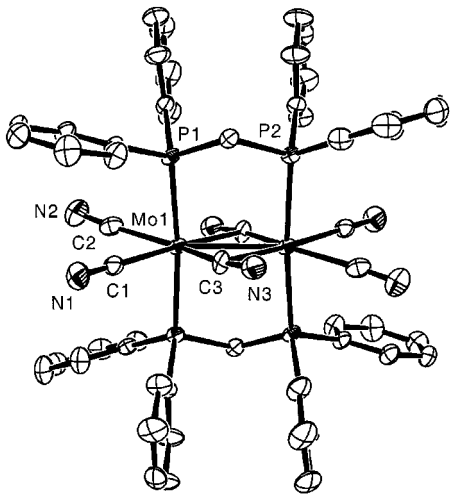

Figure 2. Thermal ellipsoid plot of the anionic unit in [*n*-Bu_4N][$Mo_2(CN)_6(dppm)_2$] (**3**·$2CH_3CN$·$2H_2O$) represented at the 50% probability level. Hydrogen atoms have been omitted for clarity.

Structures of the Related Molecules $[Mo_2(CN)_6(dppm)_2]^{2-}$, $[Mo_2(CN)_6(dppm)_2]^{1-}$, and $Mo_2(CN)_6(dppm)_2$. A single-crystal X-ray structure of **1**·$2CH_3CN$·$2C_6H_6$ was reported by us in an earlier communication.[9] The quality of the data set was poor which led to unreliable geometric parameters. We now report the structure of **2** which contains the anion $[Mo_2(CN)_6(dppm)_2]^{2-}$ crystallized as the $[Et_4N]^+$ salt. The three species, $[Mo_2(CN)_6(dppm)_2]^{2-}$, $[Mo_2(CN)_6(dppm)_2]^{1-}$, and $Mo_2(CN)_6(dppm)_2$, all possess identical ligand sets, namely two *trans*-dppm ligands which bisect an equatorial plane consisting of the unit $Mo_2(\mu\text{-}CN)_2(CN)_4$. Thermal ellipsoid plots of $[Mo_2(CN)_6(dppm)_2]^{2-}$, $[Mo_2(CN)_6(dppm)_2]^{1-}$, and $Mo_2(CN)_6(dppm)_2$ are depicted in Figures 1−3, respectively. Relevant bond distances and angles are provided in Tables 2−4.

The Mo−P distances in compounds **2**−**4** span the range 2.494(2)−2.557(1) Å, which is typical of the values reported for other dimolybdenum−diphosphine complexes.[12,26] In general, the C≡N distances (1.086(4)−1.127(4) Å) are shorter in complex **4** than the corresponding values in **2** and

(24) Glusker, J. P.; Lewis, M.; Rossi, M. *Crystal Structure Analysis for Chemists and Biologists*; VCH Publishers: New York, 1994.
(25) The values in parentheses are for ΔE_p (i.e. $E_{p,a} - E_{p,c}$) in millivolts.

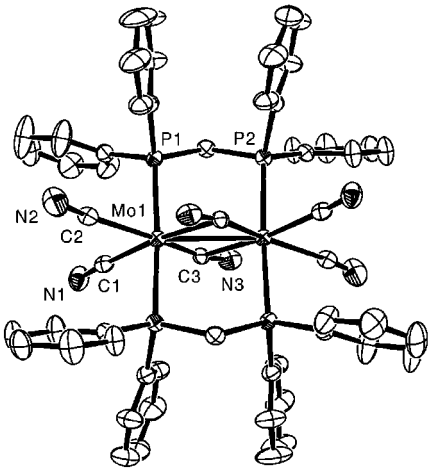

Figure 3. Thermal ellipsoid plot of the molecule $Mo_2(CN)_6(dppm)_2$ (**4**·$2CH_3NO_2$) represented at the 50% probability level. Hydrogen atoms have been omitted for the sake of clarity.

Table 2. Selected Bond Distances (Å) and Bond Angles (deg) in $[Et_4N]_2[Mo_2(CN)_6(dppm)_2]$ (**2**·$2CH_3CN$)

Bond Distances			
Mo(1)−Mo(1A)	2.7355(13)	C(1)−N(1)	1.157(8)
Mo(1)−C(1)	2.140(8)	C(2)−N(2)	1.145(8)
Mo(1)−C(2)	2.193(7)	C(3)−N(3)	1.168(8)
Mo(1)−C(3)	2.054(8)	Mo(1)−P(1)	2.494(2)
Mo(1)−C(3A)	2.288(7)	Mo(1)−P(2)	2.497(2)
Bond Angles			
C(2)−Mo(1)−C(1)	80.7(3)	Mo(1)−C(3)−N(3)	172.8(6)
C(3)−Mo(1)−C(1)	80.7(3)	Mo(1A)−C(3)−N(3)	96.5(5)
C(3)−Mo(1)−C(2)	158.5(3)	P(1)−Mo(1)−P(2)	173.14(7)

Table 3. Selected Bond Distances (Å) and Bond Angles (deg) in $[n\text{-}Bu_4N][Mo_2(CN)_6(dppm)_2]$ (**3**·$2CH_3CN$·$2H_2O$)

Bond Distances			
Mo(1)−Mo(1A)	2.8299(10)	C(1)−N(1)	1.151(5)
Mo(1)−C(1)	2.155(4)	C(2)−N(2)	1.153(6)
Mo(1)−C(2)	2.181(5)	C(3)−N(3)	1.161(5)
Mo(1)−C(3)	2.032(4)	Mo(1)−P(1)	2.537(1)
Mo(1)−C(3A)	2.252(3)	Mo(1)−P(2A)	2.542(1)
Bond Angles			
C(2)−Mo(1)−C(1)	78.47(16)	Mo(1)−C(3)−N(3)	168.2(3)
C(3)−Mo(1)−C(1)	80.75(15)	Mo(1A)−C(3)−N(3)	86.2(3)
C(3)−Mo(1)−C(2)	157.64(15)	P(1)−Mo(1)−P(2A)	174.31(3)

Table 4. Selected Bond Distances (Å) and Bond Angles (deg) in $Mo_2(CN)_6(dppm)_2$ (**4**·$2CH_3NO_2$)

Bond Distances			
Mo(1)−Mo(1A)	2.9357(9)	C(1)−N(1)	1.127(4)
Mo(1)−C(1)	2.176(4)	C(2)−N(2)	1.086(4)
Mo(1)−C(2)	2.251(3)	C(3)−N(3)	1.121(4)
Mo(1)−C(3)	2.087(4)	Mo(1)−P(1)	2.547(1)
Mo(1)−C(3A)	2.284(3)	Mo(1)−P(2A)	2.557(1)
Bond Angles			
C(2)−Mo(1)−C(1)	81.08(11)	Mo(1)−C(3)−N(3)	165.8(3)
C(3)−Mo(1)−C(1)	80.22(12)	Mo(1A)−C(3)−N(3)	82.2(2)
C(3)−Mo(1)−C(2)	159.02(12)	P(1)−Mo(1)−P(2A)	176.90(3)

3 (1.145(8)−1.168(8) Å). The higher charge on the metal atoms in complex **4** is presumably responsible for this effect.[27]

(26) (a) Lang, H. F.; Fanwick, P. E.; Walton, R. A. *Inorg. Chim. Acta* **2001**, *322*, 17. (b) Xue, W.-M.; Kühn, F. E.; Zhang, G.; Herdtweck, E.; Raudaschl-Sieber, G. *J. Chem. Soc., Dalton Trans.* **1999**, 4103. (c) Cotton. F. A.; Falvello, L. R.; Harwood, W. S.; Powell, G. L.; Walton, R. A. *Inorg. Chem.* **1986**, *25*, 3949.

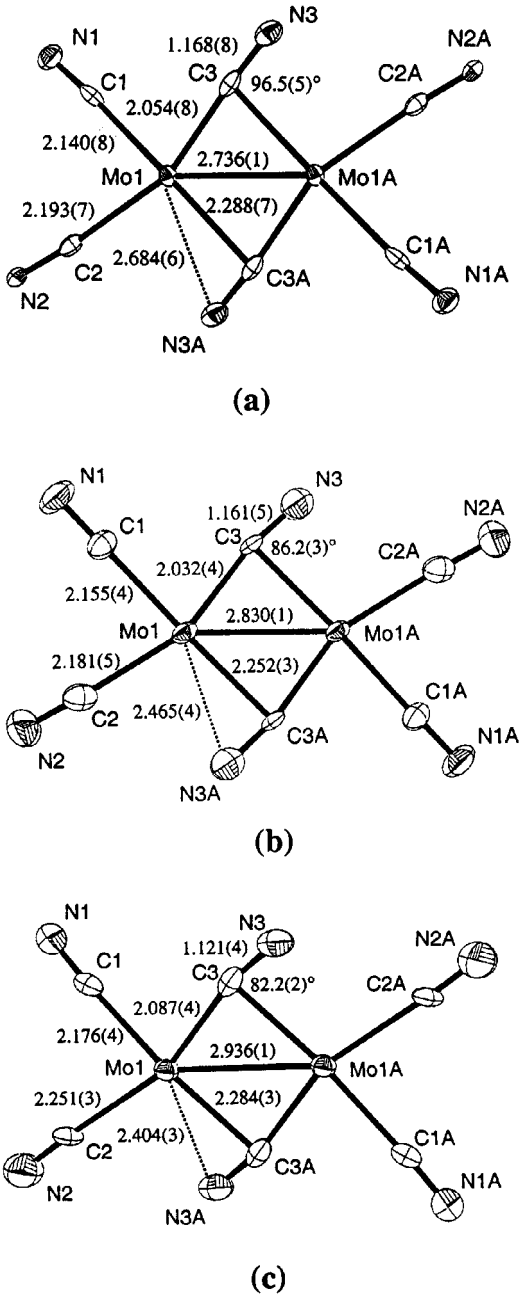

Figure 4. Comparison of the relevant metrical parameters within the $Mo_2(\mu\text{-}CN)_2(CN)_4$ units in **2**·$2CH_3CN$ (a), **3**·$2CH_3CN$·$2H_2O$ (b), and (**4**)·$2CH_3NO_2$ (c).

Despite the apparent similarities in the molecular cores of these complexes, the arrangement of the bridging cyanide ligands and the metal−metal separations reflect the different oxidation states. A plot of the $Mo_2(\mu\text{-}CN)_2(CN)_4$ units in complexes **2**−**4** is provided in Figure 4. Pertinent bond distances and angles are compiled in Table 5. A gradual increase in the Mo−Mo distances is observed as one oxidizes the $Mo_2^{II,II}$ unit in **2** to $Mo_2^{III,III}$ in **4** (2.7355(13) versus 2.9357(9) Å). An intermediate Mo−Mo distance of 2.8299(10) Å was observed for the $Mo_2^{II,III}$ unit in **3**. A careful inspection of the metrical parameters reveals the differences in the arrangement of the cyanide ligands. The bridging

(27) Bera, J. K.; Samuelson, A. G.; Chandrasekhar, J. *Organometallics* **1998**, *17*, 4136 and references therein.

Table 5. Comparison of Metrical Parameters of the $Mo_2(\mu\text{-}CN)_2(CN)_4$ Units in Complexes $[Et_4N]_2[Mo_2(CN)_6(dppm)_2]$ (**2**·$2CH_3CN$), $[n\text{-}Bu_4N][Mo_2(CN)_6(dppm)_2]$ (**3**·$2CH_3CN$·$2H_2O$), and $Mo_2(CN)_6(dppm)_2$ (**4**·$2CH_3NO_2$)

	$Mo_2^{II,II}$ (**2**)	$Mo_2^{II,III}$ (**3**)	$Mo_2^{III,III}$ (**4**)
	bond distances (Å)		
Mo(1)−Mo(1A)	2.7355(13)	2.8299(10)	2.9357(9)
Mo(1)−C(1)	2.140(8)	2.155(4)	2.176(4)
Mo(1)−C(2)	2.193(7)	2.181(5)	2.251(3)
Mo(1)−C(3)	2.054(8)	2.032(4)	2.087(4)
Mo(1)−C(3A)	2.288(7)	2.252(3)	2.284(3)
C(3)−N(3)	1.168(8)	1.161(5)	1.121(4)
Mo(1)−N(3A)	2.684(6)	2.465(4)	2.404(3)
	bond angles (deg)		
Mo(1)−C(3)−N(3)	172.8(6)	168.2(3)	165.8(3)
Mo(1)−C(3)−Mo(1A)	77.9(2)	82.5(1)	84.2(1)
Mo(1)−C(3A)−N(3A)	96.5(5)	86.2(3)	82.2(2)
C(1)−Mo(1)−C(2)	80.7(3)	78.47(16)	81.08(11)

cyanide ligands are stabilized by side-on π-interactions in the oxidized compounds **3** and **4**. The differences in the orientations of the bridging cyanide ligands in these three complexes are evident by the angles subtended by the Mo atoms and μ-CN groups (Figure 4). The Mo−C−N angles reflect electronic differences in the series. In complex **2**, the angles Mo(1)−C(3)−N(3) and Mo(1)−C(3A)−N(3A) are 172.8(6)° and 96.5(5)°, respectively. The corresponding angles are 168.2(3)° and 86.2(3)° in **3** and 165.8(3)° and 82.2(2)° in **4**, respectively. This change of angles is manifested by a considerable shortening of the Mo(1)−N(3A) distances across the series (2.684(6) Å for the $Mo_2^{II,II}$ unit in **2**, 2.465(4) Å for the $Mo_2^{II,III}$ unit in **3**, and 2.404(3) Å for the $Mo_2^{III,III}$ in **4**).

Infrared Spectral Studies. The presence of two cyanide environments in **1** was confirmed by infrared spectroscopy. The localized D_{2h} symmetry of the four terminal cyanide ligands is expected to give rise to two IR active vibrational modes. The ν(C≡N) modes occur at 2094 and 2080 cm^{-1} for the terminal cyanides and at 1936 cm^{-1} for the bridging cyanides.

Although both **1** and **3** exhibit similar ESBO structures, the infrared spectrum of **3** displays two ν(C≡N) stretches at 2108 and 1807 cm^{-1}. The lack of a second stretch in the higher energy region is presumably due to the fact that the symmetric and antisymmetric stretches for the four terminal cyanides are degenerate. The ν(C≡N) mode for the bridging cyanide appears at 1807 cm^{-1} in complex **3** which is 129 cm^{-1} lower than the ν(C≡N) stretches of the μ-(CN) groups in **1**. The corresponding ν(C≡N) modes of **4** occur at 2110 and 2102 cm^{-1} (terminal) and 1807 cm^{-1} (bridging). The pronounced decrease in the ν(C≡N) bridging mode from 1936 cm^{-1} in **1** to 1807 cm^{-1} in **3** and **4** is symptomatic of the differences observed in the bridging cyanide bonding in **1** versus **3** and **4**. It is important to point out that if only the charges on the Mo_2 unit were considered, an increase in ν(C≡N) upon oxidation would be expected because of decreased dπ(Mo) → pπ*(CN) back-bonding. As already mentioned, the X-ray structures of complexes **2** and **3** reveal that the bridging cyanides are leaning over in such as way that the π-orbitals of the CN unit can donate into empty metal-based orbitals which results in a weakening of the C≡N bond and hence a decrease of the ν(C≡N) mode. The similarity in the Mo−C≡N angles in complexes **3** and **4** (see Table **5**) indicates that the extent of the π-interaction in these complexes is comparable, a situation that is reflected in the energies of the bridging ν(C≡N) mode, namely ∼1807 cm^{-1} for both compounds.

^{1}H and ^{31}P{^{1}H} NMR Spectroscopy. The ^{1}H NMR spectrum of **1** is typical of a diamagnetic compound with a symmetrical *trans*-$M_2(dppm)_2$ core.[28] The ^{1}H NMR resonances for the bridgehead methylene protons of the dppm ligand appear as a pentet centered at δ 4.08 ppm which arises from virtual coupling of the methylene protons with four equivalent P nuclei. Multiplets for the phenyl groups of the dppm units are observed at δ 7.60 and 6.96 ppm along with resonances that correspond to methyl and methylene protons of tetra-*n*-butylammonium groups. The ^{31}P{^{1}H} spectrum of **1** consists of a sharp singlet located at δ 25.5 ppm.

In accord with the assignment of the mixed valence $Mo_2^{II,III}$ core, the ^{1}H NMR spectrum of **3** contains only broad signals indicative of paramagnetism. Likewise, the ^{31}P NMR spectrum of **3** was featureless. Unfortunately, the poor solubility of **4** prevented analysis by NMR methods.

Electronic Spectroscopy. The d−d transitions for **1** were observed to occur at 553 and 333 nm with ϵ values of 1.9×10^3 and 3.4×10^5 L mol^{-1} cm^{-1}, respectively. The corresponding transitions for **3** occur at 420 (800 L mol^{-1} cm^{-1}) and 780 nm (1.2×10^3 L mol^{-1} cm^{-1}). The differences in the electronic properties allow for ease in verifying that samples of **3** are not contaminated with **1**. The insolubility of samples of **4**, once it has been isolated as a pure crystalline material, precluded a UV−vis spectroscopic analysis.

Metal−Metal Bonding Considerations. The qualitative picture of the orbital interactions in metal−metal bonded compounds, established by F. A. Cotton many years ago,[29] has been supplemented by a number of high-level theoretical calculations in recent years.[30] Whenever possible, it is convenient to test the bonding models by examining the variations in M−M distances among M_2 complexes with the identical ligand sets and molecular geometries.[11] The current set of compounds $[Mo_2(CN)_6(dppm)_2]^{2-/1-/0}$ is a new type of homologous ESBO series that contains Mo_2 units in three different core oxidation states, viz., $Mo_2^{II,II}$, $Mo_2^{II,III}$, and $Mo_2^{III,III}$. This situation presents us with a unique opportunity to study the variation of Mo−Mo distances with depopulation of the HOMO orbital of the compound $[Mo_2(CN)_6(dppm)_2]^{2-}$.

Any discussion of how one would expect the Mo−Mo distances in these compounds to change with d electron count must necessarily begin with a review of the general bonding in ESBO compounds. According to the established MO scheme for ESBO complexes, only one set each of σ, π,

(28) Barder, T. J.; Cotton, F. A.; Lewis, D.; Schwotzer, W.; Tetrick, S. M.; Walton, R. A. *J. Am. Chem. Soc.* **1984**, *106*, 2882.
(29) Cotton, F. A.; Curtis, N. F.; Harris, C. B.; Johnson, B. F. G.; Lippard, S. J.; Mague, J. T.; Robinson, W. R.; Wood, J. S. *Science*, **1964**, *145*, 1305.
(30) (a) Cotton, F. A.; Feng, X. *J. Am. Chem. Soc.* **1998**, *120*, 3387. (b) Cotton, F. A.; Feng, X. *J. Am. Chem. Soc.* **1997**, *119*, 7514.

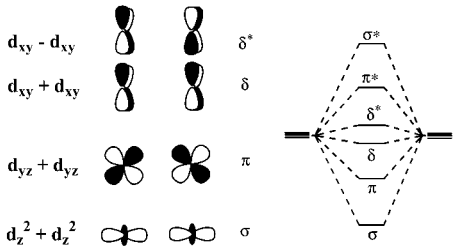

Figure 5. Schematic representation of the orbital overlap patterns involved in M−M bonding in ESBO complexes.

and δ orbitals is involved in the M−M bonding interaction.[31] A schematic representation of the bonding and antibonding interactions of these orbitals is shown in Figure 5. Because the relative ordering of the δ and δ^* levels in these compounds is ambiguous,[10] it is best to write the electronic configurations for the $Mo_2^{II,II}$, $Mo_2^{II,III}$, and $Mo_2^{III,III}$ compounds in a general fashion, viz., $\sigma^2\pi^2(\delta\delta^*)^4$, $\sigma^2\pi^2(\delta\delta^*)^3$, and $\sigma^2\pi^2(\delta\delta^*)^2$, respectively, with no emphasis being placed on whether δ or δ^* is actually lower in energy.[10,11]

Computational Studies of $[Mo_2(CN)_6(dppm)_2]^{2-}$ and $Mo_2(CN)_6(dppm)_2$. Because it is not useful to assign formal bond orders in ESBO compounds with a HOMO level of the δ/δ^* types, we turned to a theoretical study to help explain the Mo−Mo variations in the series. X-ray studies reveal that the Mo−Mo distances increase from 2.736(1) Å in $Mo_2^{II,II}$ to 2.830(1) Å in $Mo_2^{II,III}$ and to 2.936(1) Å in $Mo_2^{III,III}$. The question that we posed at this point is the following: What role, if any, do interactions between the semibridging cyanides and the d−d MOs of the Mo−Mo unit play in tuning the metal−metal bonding in these compounds? To answer this question, computational studies were undertaken on the closed-shell members of the series $[Mo_2(CN)_6(dppm)_2]^{2-}$ and $Mo_2(CN)_6(dppm)_2$. Geometrical parameters were taken from the X-ray structures of **2** and **4**, respectively.

Contour diagrams of the frontier orbitals of **2** ($Mo_2^{II,II}$) and **4** ($Mo_2^{III,III}$) are depicted in Figure 6. The HOMO (no. 76) of the $Mo_2^{II,II}$ system resembles a δ orbital resulting primarily from a bonding interaction between metal d_{xy} orbitals. The p_x orbitals of N3A (and N3) are involved in an antibonding interaction with the δ orbital (Figure 6a). The HOMO − 1 (no. 75) is predominantly a metal-based δ^* orbital arising from an out-of-phase interaction of d_{xy} orbitals on the metal atoms. No contribution from the p_x orbitals of N3 and N3A was observed (Figure 6b). It is important to point out, however, that the δ and δ^* orbitals (HOMO and HOMO − 1) are virtually degenerate with a separation of less than ∼0.4 kcal/mol.

The HOMO (no. 75) of the $Mo_2^{III,III}$ compound **4** is a δ^* orbital (Figure 6d), and the LUMO (No. 76) is a δ orbital (Figure 6c); these are separated by ∼26 kcal/mol. The coefficients of the atomic orbitals indicate that the HOMO for **2** and LUMO of **4** are of similar parentage as are the HOMO − 1 of **2** and the HOMO of **4**.

(31) (a) Shaik, S.; Hoffmann, R.; Fisel, C. R.; Summerville, R. H. *J. Am. Chem. Soc.* **1980**, *102*, 4555. (b) Shaik, S.; Hoffmann, R. *J. Am. Chem. Soc.* **1980**, *102*, 1194.

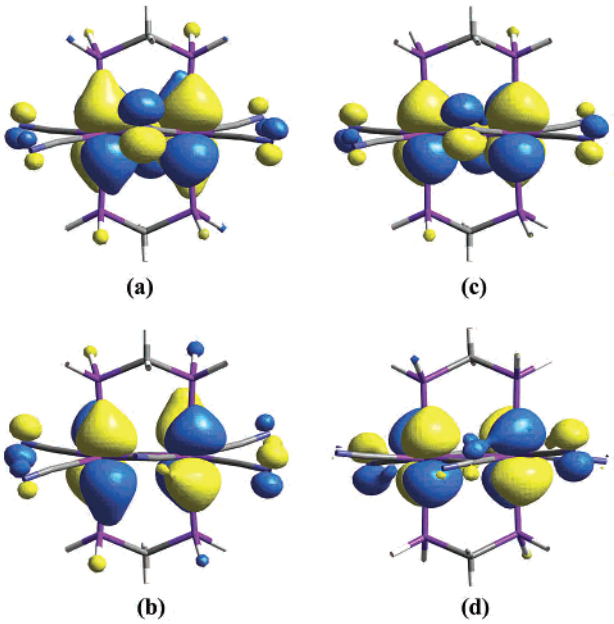

Figure 6. Contour diagrams of the (a) HOMO and (b) HOMO − 1 of the $Mo_2^{II,II}$ unit in **2** and the (c) LUMO and (d) HOMO of the $Mo_2^{III,III}$ unit in **4**.

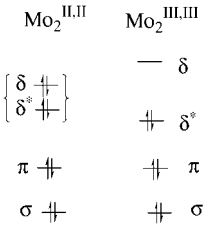

Figure 7. Comparison of the filling of the molecular orbital levels involved in the M−M bonding in $[Et_4N]_2[Mo_2(CN)_6(dppm)_2]$ (**2**) and $Mo_2(CN)_6(dppm)_2$ (**4**) as indicated by the DFT calculations.

These DFT calculations support the conclusion that a two-electron oxidation of the $Mo_2^{II,II}$ core to $Mo_2^{III,III}$ leads to a destabilization of the δ orbital. This situation arises because of improved antibonding overlap of the p_x orbitals on N3A (and N3) with the δ orbital (Figure 6c), thereby leading to a destabilization of this orbital. This improved orbital overlap is due to shorter Mo1−N3A (and Mo1A −N3) distances and Mo1−C3A−N3A (and Mo1A−C3−N3) angles in $Mo_2^{III,III}$ compared to the corresponding distances and angles in $Mo_2^{II,II}$ (Table 5). The semibridging orientation of the bridging cyanide helps to stabilize the δ^* orbital, albeit marginally, as a consequence of favorable overlap of the p_x orbital on the C3A (and C3) with the metal-based δ^* orbital (Figure 6d). This type of interaction is not present significantly in complex **1**. The end result is that the closely spaced δ and δ^* levels of the $Mo_2^{II,II}$ compound, upon two-electron oxidation, become well separated; the filled δ level of the $Mo_2^{II,II}$ compound is destabilized by oxidation and becomes the empty LUMO for $Mo_2^{III,III}$, and the δ^* orbital becomes the HOMO for the fully oxidized $Mo_2^{III,III}$ compound. The net result is that the occupation of the molecular orbitals involved in the M−M bonding in $[Et_4N]_2[Mo_2(CN)_6(dppm)_2]$ (**2**) and $Mo_2(CN)_6(dppm)_2$ (**4**) is $\sigma^2\pi^2(\delta\delta^*)^4$ and $\sigma^2\pi^2\delta^{*2}\delta^0$, respectively (Figure 7). The loss of the δ bonding contribution to the metal−metal bond contributes to an increase in

the Mo−Mo distance in going from the $Mo_2^{II,II}$ species to the $Mo_2^{III,III}$ compound.

It is important to point out that, in discussions of M−M bond variations in a series such as this one, the role of increased positive charge on the metals must also be considered. Oxidation leads to orbital contraction and less overlap, the ultimate result of which is longer M−M distances. It is reasonable to conclude that a combination of the effects of increased charge *and* donation from the semibridging cyanide into a primarily δ^* level leads to the significant bond lengthening observed in the X-ray structures.

Conclusions

Reactions of $Mo_2Cl_4(dppm)_2$ with [*n*-Bu_4N][CN] or [Et_4N][CN] proceed with complete displacement of the four chloride ligands and addition of two cyanides to yield the new compound $[Mo_2^{II,II}(CN)_6(dppm)_2]^{2-}$ which is readily oxidized by $NOBF_4$ to the one- and two-electron oxidation products $[Mo_2^{II,III}(CN)_6(dppm)_2]^{1-}$ and $Mo_2^{III,III}(CN)_6(dppm)_2$. X-ray studies reveal that the oxidation state of the dimolybdenum core influences the bonding interactions of the bridging cyanides as well as the Mo−Mo distances. The side-on π-donation of the bridging cyanides to the metal centers in oxidized compounds **3** and **4** is more pronounced than it is in the parent compound, **2**. The results of DFT calculations indicate that the δ and δ^* orbitals are nearly degenerate in the parent compound $[Et_4N]_2[Mo_2^{II,II}(CN)_6(dppm)_2]$ (**2**) while increased interactions of the semibridging cyanides with metal orbitals in $Mo_2^{III,III}(CN)_6(dppm)_2$ (**4**) lead to well-separated δ and δ^* levels. The filled δ level of the $Mo_2^{II,II}$ compound is destabilized by oxidation and becomes the empty LUMO for $Mo_2^{III,III}$, and the δ^* orbital become the HOMO for the fully oxidized $Mo_2^{III,III}$ compound. The loss of the δ bonding contribution to the metal−metal bond combined with the reduced orbital overlap due to higher charge on metal centers contributes to an increase in the Mo−Mo distance in going from the $Mo_2^{II,II}$ to the $Mo_2^{III,III}$ compound.

Acknowledgment. The authors gratefully acknowledge the National Science Foundation (PI Grant, NSF CHE-9906583; CCD diffractometer, CHE-9807975) as well as the Welch Foundation (A-1449) for support of this project. We also thank Dr. Lisa Thomson of the Laboratory for Molecular Simulation (LMS) in the Chemistry Department at Texas A&M University for helpful discussions.

Supporting Information Available: Crystallographic data in CIF format. This material is available free of charge via the Internet at http://pubs.acs.org.

IC020157N